Drug Development and Industrial Pharmacy, 2011; 37(6): 714–718

ISSN 0363-9045 print/ISSN 1520-5762 online
DOI: 10.3109/03639045.2010.538059

informa
healthcare

RESEARCH ARTICLE

The controlled release of tilmicosin from silica nanoparticles

Meirong Song[1], Yanyan Li[2], Cailing Fai[1], Shumin Cui[1], and Baoan Cui[1]

[1]College of Sciences, Henan Agricultural University, Zhengzhou, P. R. China, and [2]Department of Education, Henan Institute of Science and Technology, Xinxiang, P. R. China

Abstract

The aim of this study was to use silica nanoparticles as the carrier for controlled release of tilmicosin. Tilmicosin was selected as a drug model molecule because it has a lengthy elimination half-life and a high concentration in milk after subcutaneous administration. Three samples of tilmicosin-loaded silica nanoparticles were prepared with different drug-loading weight. The drug-loading weight in three samples, as measured by thermal gravimetric analysis, was 29%, 42%, and 64%, respectively. With increased drug-loading weight, the average diameter of the drug-loaded silica nanoparticles was increased from 13.4 to 25.7 nm, and the zeta potential changed from−30.62 to−6.78 mV, indicating that the stability of the drug-loaded particles in the aqueous solution decreases as drug-loading weight increases. *In vitro* release studies in phosphate-buffered saline showed the sample with 29% drug loading had a slow and sustained drug release, reaching 44% after 72 h. The release rate rose with increased drug-loading weight; therefore, the release of tilmicosin from silica nanoparticles was well-controlled by adjusting the drug loading. Finally, kinetics analysis suggested that drug released from silica nanoparticles was mainly a diffusion-controlled process.

Keywords: Silica nanoparticles, tilmicosin, controlled release, diffusion, nanomaterials

Introduction

Tilmicosin ($C_{46}H_{80}N_2O_{13}$, 20-deoxo-20-(3,5-dimethyl-1-piperidinyl)desmycosin) is a 16-membered ring, semisynthetic macrolide antibiotic drug[1], and its molecular structure is shown in Figure 1. Tilmicosin is recommended for treatment and prevention of pneumonia and mastitis in cattle, sheep, and pigs. But it has properties with a distribution volume large and serum long half-life[2]. After subcutaneous administration, tilmicosin rapidly accumulates in bovine macrophages and mammary gland epithelial cells[3], and has long elimination half-life and high concentration in milk[4,5]. Furthermore, high dose of tilmicosin has some side effects such as cardiotoxic effect, anaphylaxis, collapse, and transient swelling at the injection site[6–9]. To solve these problems, it was formulated to release tilmicosin in a designed controlled fashion to achieve and maintain concentrations above the lung minimum concentration inhibitory (MIC), following a single 10 mg/kg body weight (BW) after subcutaneous injection. Zhou and colleagues developed the hydrogenated castor oil (HCO)–solid lipid nanoparticle (SLN) system as tilmicosin carrier for controlled and sustained release[2]. One disadvantage of this approach is that oil only rarely provides the solubilizing power to dissolve the required dose in a reasonable quantity of oil. This limits the option of using a simple drug/oil formulation system[10].

In this study, a silica sol consisting of spherical silica nanoparticles dispersed in aqueous solution was used as the carrier for controlled tilmicosin release. This system includes many advantages of silica carriers, such as high levels of chemical and thermal stability, easily modified surface properties, large surface area, good biocompatibility, and favorable tissue response[11–20]. In addition, the silica nanoparticles are conventionally made by using a sodium silicate solution called water glass as starting material and it is very cheap. Finally, the huge specific surface of silica nanoparticles will not be wasted as a result of conglomeration since they are well-dispersed in aqueous solution.

Address for Correspondence: Baoan Cui, Henan Agricultural University, Zhengzhou 450002, P. R. China. E-mail: smr770505@yahoo.com.cn

(Received 21 June 2010; revised 30 October 2010; accepted 01 November 2010)

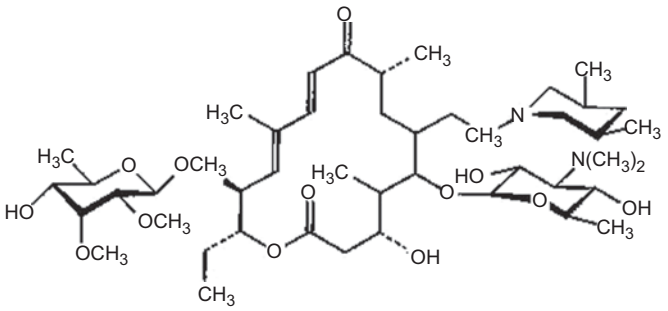

Figure 1. Molecular structure of tilmicosin.

Materials and methods

Materials

Silica sol with a silica concentration of 25 wt% was supplied by Zhengzhou Jingwei Composite Material Co. Ltd. Tilmicosin (>200 nm) was supplied by Henan Biyun Days Animal Pharmaceutical Co. Sodium dihydrogen phosphate (NaH_2PO_3) and sodium hydrogen phosphate (Na_2HPO_3) were of analytical grade and were used as received.

Drug loading

In a typical drug-loading process, tilmicosin was first dissolved in ethanol to a concentration of 37.5 wt%. A known volume of silica sol was added drop wise into the solution of tilmicosin, which was stirred continuously by a magnetic follower at room temperature. A milk-white suspension appeared and the process was allowed to continue for 20 min to ensure maximum drug loading. The white material was collected by centrifugation, washed with water, dried in air at 37°C for 24 h, and finally ground to a white powder in a ceramic pestle and mortar. The theoretical drug-loading weight was calculated according to the following equation.

$$\text{Theoretical drug-loading weight} = \frac{x \times 37.5\%}{x \times 37.5\% + y \times 25\%}$$

Here, x is the mass of tilmicosin solution and y is the mass of silica sol. By changing the input amounts of tilmicosin and silica sol, the theoretical drug-loading weight of the silica nanoparticles in the three samples named TS1, TS2, and TS3 was 20, 40, and 60 wt%, respectively.

Characterization

The zeta potential and size distribution of tilmicosin-loaded silica nanoparticles were measured with a zetasizer Nano-ZS90 laser particle size analyzer. TS1 was observed by transmission electron microscopy (TEM) with a JEM 2100 instrument. The actual drug-loading weight was determined with an American Diamond thermal gravimetric analyzer (TGA). Colloidal particles of silica sol were collected by centrifugation and dried for comparison. The samples were heated at a rate of 10°C/ min in a stream of nitrogen gas. The Fourier transform infrared (FTIR) spectrum was obtained with a CARY Eclipse FTIR spectrophotometer.

In vitro release studies

A known amount of tilmicosin-loaded nanoparticles was suspended in 2 mL of phosphate-buffered saline (PBS, pH 7.4) in a dialysis bag and dialyzed against 30 mL of PBS at 37°C, which was stirred continuously by a magnetic follower. The amount of drug-loaded nanoparticles depended on the loading weight in order to ensure the drug content was 0.24 g. To determine the amount of tilmicosin that diffused through the dialysis bag, samples (0.5 mL) were withdrawn from the receiver solution and the same amount of fresh medium was added to the receiver at fixed time points. The sample was diluted 200-fold with PBS. The concentration of tilmicosin released into solution as a function of time was determined from measurement of the absorbance at 291 nm (CARY 300 spectrophotometer), the characteristic absorption wavelength of tilmicosin in PBS[21]. Tilmicosin standards were prepared by dissolving weighed amounts of the drug in PBS. For comparison, dissolution of tilmicosin alone was investigated under the same conditions and all experiments were done in triplicate. The *in vitro* method is to learn from reference[15].

Results and discussion

Size and zeta potential

Table 1 shows the size and zeta potential of tilmicosin-loaded silica nanoparticles and silica nanoparticles alone as determined by a zetasizer laser particle size analyzer. Silica nanoparticles were negatively charged and have an average diameter of ~6.8 nm. The high absolute value of the zeta potential (44.80 mV) confered good stability to the silica nanoparticles. After adsorption of tilmicosin molecules, the silica nanoparticles increased in size from 13.4 to 25.7 nm, and the absolute value of the zeta potential decreased (from –30.62 to –6.78 mV) with increased drug-loading weight.

The significance of zeta potential is that its value can be related to the stability of colloidal dispersions. Colloids with high zeta potential (negative or positive) are electrically stabilized because of the large repulsion between adjacent, similarly charged particles in dispersion.

Table 1. The size and zeta potential of tilmicosin-loaded silica particles and silica sol as determined by zetasizer laser particle size analyzer.

Sample	Silica sol	TS1	TS2	TS3
Zeta potential	−44.80 mV	−30.62 mV	−18.65 mV	−6.78 mV
Average size	~6.8 nm	~13.4 nm	~21.2 nm	~25.7 nm

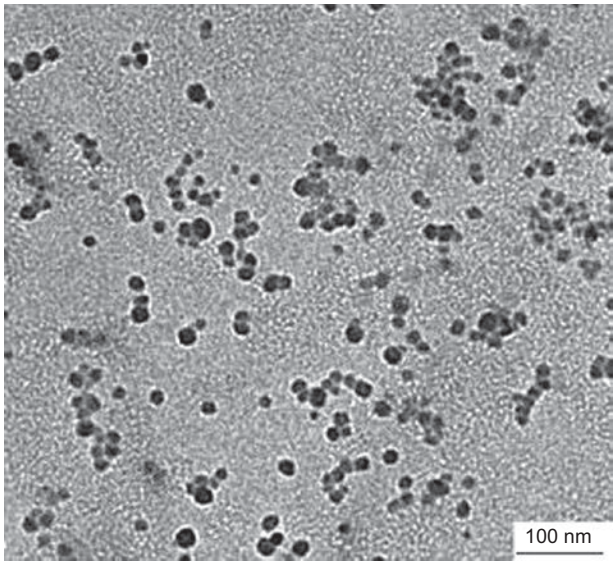

Figure 2. Transmission electron microscopic (TEM) image of TS1.

According to the zeta potential of the three samples, the stability of the drug-loaded particles in the aqueous solution decreases as drug-loading weight increases; that is, TS1 has the moderate stability, whereas the other two samples are unstable and tend to congregate and precipitate. TEM image of TS1 was investigated to demonstrate the results as shown in Figure 2. It was found that the sample TS1 has the moderate stability and there is no serious congregation occurring.

Drug adsorption

The FTIR spectrum of tilmicosin-loaded silica nanoparticles was obtained and compared with that of pure tilmicosin, tilmicosin after the same treatment without the carrier, and the silica nanoparticles alone (Figure 3). The characteristic peaks of drug-loaded silica nanoparticles are identical with those of silica and tilmicosin alone[22–24], except for the overlapping region at lower wave numbers between 1000 and 1400 cm^{-1}, where a broad absorption peak is found that might be the integrated adsorption of silica and tilmicosin. In addition, the FTIR spectrum of the drug following the same treatment without the carrier is identical with that of the original drug as shown in Figure 3. These results indicate that the drug has been adsorbed onto the carrier and no degradation of drug occurred during the loading procedure.

The loading weight percentage (W) of tilmicosin loaded onto silica nanoparticles was determined by TGA (Figure 4). From the TGA profile of tilmicosin alone, it is clear that the drug molecules were totally decomposed at a temperature >800°C. For silica nanoparticles

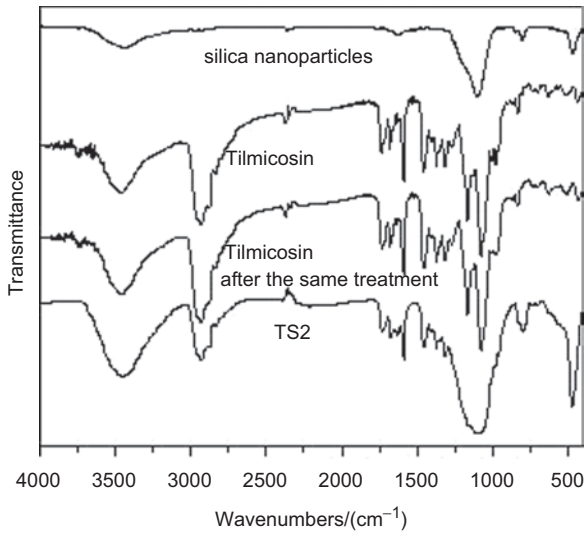

Figure 3. The Fourier transform infrared (FTIR) spectra of tilmicosin, tilmicosin after the same treatment without the carrier, silica nanoparticles, and tilmicosin-loaded silica particles (TS2).

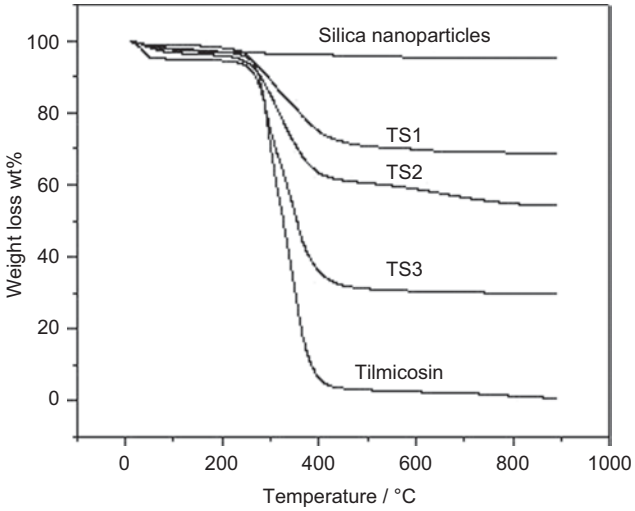

Figure 4. Thermal gravimetric analyzer (TGA) profiles of tilmicosin, silica nanoparticles, and tilmicosin-loaded silica particles.

alone, the TGA profile showed no significant weight loss at a temperature >200°C. Therefore, the weight loss of tilmicosin-loaded silica particles between 200°C and 800°C can be determined approximately as the loading weight percentage (W) of tilmicosin in the silica nanoparticles. The experimental loading weight percentage was 29 wt% for TS1, 42 wt% for TS2, and 64 wt% for TS3. In addition, it was found that the drug decomposed more slowly with reduced drug-loading weight. This phenomenon indicates that a stronger force, for example, a hydrogen bond, might exist between tilmicosin and the silica carrier.

Based on the above results, tilmicosin molecule might be adsorbed via the interactions of hydrophile groups (–OH and–C=O groups as shown in Figure 1) of drug and–OH groups on silica nanoparticles. These silica

nanoparticles acted as seeds to attract more drug molecules to grow on their surface, and they became unstable and tend to congregate and precipitate. Therefore, the drug-loaded particles became larger and larger with increased drug-loading weight, and their stability decreases as drug-loading weight increases

Drug release

In vitro release profiles of tilmicosin from samples TS1, TS2, and TS3, as well as the pure drug are shown in Figure 5. For TS1, the release curve showed a slow and sustained drug release, reaching 44% after 72 h. The release rate rose with increased loading weight. The cumulative release of TS2 reached 64% after 72 h. Tilmicosin alone showed a burst release within the first 17 h, reaching 66%, followed by a sustained release, reaching 91% after 50 h. In the case of TS3, the release rate of tilmicosin from the carrier was faster than the rate of the drug alone. The burst release was more obvious, reaching 84% in 17 h, followed by a sustained release. It is clear from these results that the release of tilmicosin from silica nanoparticles is well-controlled by adjusting the drug-loading weight.

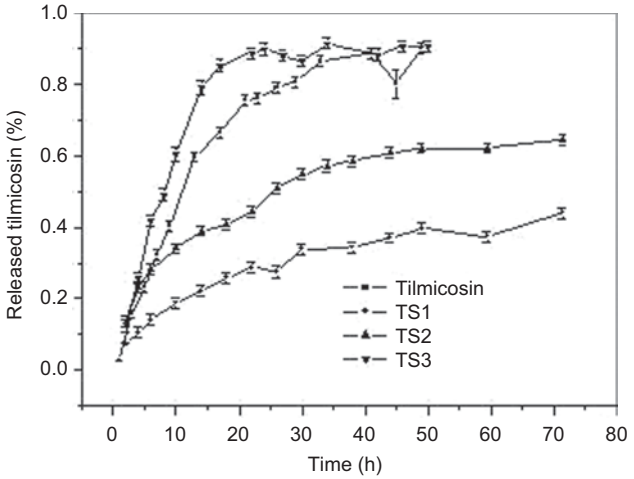

Figure 5. *In vitro* release profiles of tilmicosin released from three samples and tilmicosin alone. Error bars represent the standard deviation.

The releasing rate might be related with two spects. The first is the adsorption of the carrier, and the second is the surface area of the nanoparticles. When it comes to the drug molecules directly adsorbed by silica nanoparticles, the release fluid must moist the carrier causing desorption of the drug molecules before the drug is released from the surface of the silica nanoparticles and diffuses away. This spect lowers the releasing rate. While for drug molecules on the surface of the drug-loaded particles, their dissolution is related to the surface area to a larger extent. The larger the surface area, the faster the dissolution rate. The sample with the lowest drug-loading weight, that is, TS1, released tilmicosin at a lowest rate because the drug molecules directly adsorbed on silica nanoparticles are major. The sample with the highest drug-loading weight, that is, TS3, released at a faster rate because drug molecules adsorbed on the drug-loaded particles are major. Compared with the original drug particles (>300 nm), surface area of TS3 increased greatly. Therefore, it released tilmicosin at a fastest rate.

To analyze the mechanism of drug release from silica, data obtained from the drug-release studies were analyzed according to equations of the zero-order model, first-order model, and the Ritger–Peppas order, respectively. The regression functions and correlation coefficients of the first-order model used to fit the experimental data over the full release duration are given in Table 2. The correlation (R^2) was used as an indicator of the best fitting for each of the model considered. It is found that the first-order kinetics model performed better than the other models, indicating that the results are in accordance with the commonly used description of a diffusion-controlled process. The pharmaceutical preparation follows this dissolution profile, releasing the drug in proportion to the amount of drug remaining in its interior, such that the amount of drug released per unit time decreased[25].

Table 2. The functions and the correlation coefficients of zero-order model, first-order model, and the Ritger–Peppas order to fit the experimental data.

	Zero order		first order		Ritger–Peppas	
Sample	Functions	R^2	Functions	R^2	Functions	R^2
Tilmicosin	$\frac{M}{M_\infty} = 0.0135t+0.4079$	0.6322	$\frac{M}{M_\infty} = 0.88961 - 0.96943e^{-t/12.16559}$	0.98989	$\frac{M}{M_\infty} = 0.132t^{0.5641}$	0.8566
TS1	$\frac{M}{M_\infty} = 0.0049t+0.1347$	0.8741	$\frac{M}{M_\infty} = 0.91188 - 1.07432e^{-t/7.526429}$	0.98618	$\frac{M}{M_\infty} = 0.0575t^{0.4922}$	0.9824
TS2	$\frac{M}{M_\infty} = 0.0069t+0.265$	0.8235	$\frac{M}{M_\infty} = 0.66317 - 0.54515e^{-t/20.63939}$	0.98633	$\frac{M}{M_\infty} = 0.1229t^{0.4193}$	0.9674
TS3	$\frac{M}{M_\infty} = 0.0166t+0.2415$	0.7875	$\frac{M}{M_\infty} = 0.43776 - 0.38534e^{-t/24.7717}$	0.98236	$\frac{M}{M_\infty} = 0.0532t^{0.8141}$	0.9112

$\frac{M}{M_\infty}$ is the fraction of tilmicosin released.

Conclusions

First, the antibiotic tilmicosin was successfully loaded onto silica nanoparticles. Second, the release of tilmicosin from the silica nanoparticles was well-controlled by adjusting the drug loading. The greater the drug-loading weight, the faster the release rate. Finally, the kinetics analysis suggested that drug release from the silica sol was mainly a diffusion-controlled process.

Declaration of interest

This work was supported by the National Natural Science Foundation of China (grant number 50701016), key project in the national science and technology (2006BAD06A08) of China, the doctoral foundation (30700351), and the personnel postdoctoral management fees (10400012) from Henan Agricultural University. The authors report no declarations of interest.

References

1. Susan LHG, Tucker DT, Robin SR. (1993). A study of tilmicosin residues in milk following subcutaneous administration to lactating dairy cows. Can Vet J 34:619–621.
2. Han C, Qi CM, Zhao BK, Cao J, Xie SY, Wang SL, Zhou WZ. (2009). Hydrogenated castor oil nanoparticles as carriers for the subcutaneous administration of tilmicosin: *in vitro* and *in vivo* studies. J Vet Pharmacol Ther 32:116–123.
3. Nickerson SC, Owens WE, Fox LK, Scheifinger CC, Shryock TR, Spike TE. (1999). Comparison of tilmicosin and cephapirin as therapeutics for *Staphylococcus aureus* mastitis at dry-off. J Dairy Sci 82:696–703.
4. Ziv G, Shem-Tov M, Glickman A, Winkler M, Saran A. (1995). Tilmicosin antibacterial activity and pharmacokinetics in cows. J Vet Pharmacol Ther 18:340–345.
5. Ramadan A. (1997). Pharmacokinetics of tilmicosin in serum and milk of goats. Res Vet Sci 62:48–50.
6. Jordan WH, Byrd RA, Cochrane RL, Hanasono GK, Hoyt JA, Main BW, Meyerhoff RD, Sarazan RD. (1993). A review of the toxicology of the antibiotic MICOTIL 300. Vet Hum Toxicol 35:151–158.
7. McGuigan MA. (1994). Human exposures to tilmicosin (MICOTIL). Vet Hum Toxicol 36:306–308.
8. Van Donkersgoed J, Dubeski PL, VanderKop M, Aalhus JL, Bygrove S, Starr WN. (2000). The effect of animal health products on the formation of injection site lesions in subprimals of experimentally injected beef calves. Can Vet J 41:617–622.
9. Clark C, Woodbury M, Dowling P, Ross S, Boison JO. (2004). A preliminary investigation of the disposition of tilmicosin residues in elk tissues and serum. J Vet Pharmacol Ther 27:385–387.
10. Milan S, Stanislav Ž. (2001). Lipid-based vehicle for oral drug delivery. Biomed Papers 145:17–26.
11. Radin S, Chen T, Ducheyne P. (2009). The controlled release of drugs from emulsified, sol gel processed silica microspheres. Biomaterials 30:850–858.
12. Prokopowicz M. (2009). Correlation between physicochemical properties of doxorubicin-loaded silica/polydimethylsiloxane xerogel and *in vitro* release of drug. Acta Biomater 5:193–207.
13. Guenther U, Smirnova I, Neubert RH. (2008). Hydrophilic silica aerogels as dermal drug delivery systems—dithranol as a model drug. Eur J Pharm Biopharm 69:935–942.
14. Slowing II, Vivero-Escoto JL, Wu CW, Lin VS. (2008). Mesoporous silica nanoparticles as controlled release drug delivery and gene transfection carriers. Adv Drug Deliv Rev 60:1278–1288.
15. Xu W, Gao Q, Xu Y, Wu D, Sun Y. (2009). pH-Controlled drug release from mesoporous silica tablets coated with hydroxypropyl methylcellulose phthalate. Mater Res Bull 44:606–612.
16. Lin CX, Qiao SZ, Yu CZ, Ismadji S, Lu G.Q. (2009). Periodic mesoporous silica and organosilica with controlled morphologies as carriers for drug release. Micropor Mesopor Mat 117: 213–219.
17. Musa EB, Ala'a E, Iyad R, Mayyas AR, Adnan B. (2008). A novel super disintegrating agent made from physically modified chitosan with silicon dioxide. Drug Dev Ind Pharm 34:373–383.
18. Unger K, Rupprecht H, Valentin B, Kircher W. (1983). The use of porous and surface modified silica as drug delivery and stabilizing agents. Drug Dev Ind Pharm 9:69–91.
19. Branka R, Mirjam G, Mirjana G, Karine P, Franciose F. (2010). Dual influence of colloidal silica on skin deposition of vitamins C and E simultaneously incorporated in topical microemulsions. Drug Dev Ind Pharm 36:852–860.
20. Manja A, Pirjo K, Ilkka K, Juha K, Antti Y. (1999). *In vitro* release behavior of toremifene citrate from sol–gel processed sintered silica xerogels. Drug Dev Ind Pharm 25:955–959.
21. Song YH, Bai XH, Li YJ. (2005). Determination of tilmicosin by ultraviolet spectrophotometry. Shanxi Med Univ 36:71–73.
22. Zhu YF, Shi JK, Li YS, Chen HR, Shen WH, Dong XP. (2005). Hollow mesoporous spheres with cubic pore network as a potential carrier for drug storage and its *in vitro* release kinetics. J Mater Res 20: 54–61.
23. Serra L, Doménech J, Peppas NA. (2006). Drug transport mechanisms and release kinetics from molecularly designed poly(acrylic acid-*g*-ethylene glycol) hydrogels. Biomaterials 27:5440–5451.
24. Manuel D, Kevin EW, Herbert AK, Julie AW, Gary DC, Eddie VT, Jeffery TV, Fred TC, John LO, Earl EO, Satoshi O. Synthesis and antimicrobial evaluation of 20-deoxo-20-(3,5-dimethyl-1-piperidinyl)desmycosin desmycosin (tilmicosin, EL-870) and related cyclic amino derivatives. J Antibiot 62:1253–1267.
25. Costa P, Lobo JMS. (2001). Modeling and comparison of dissolution profiles. Eur J Pharm Sci 13:123–133.